JOURNAL OF MATERIALS SCIENCE 21 (1986) 2528–2534

Environmentally-affected indentation fracture in poly(ethersulphone) and poly(methyl methacrylate)

M. K. OMAR*, A. G. ATKINS
Engineering Department, University of Reading, Reading, RG6 2AY, UK
J. K. LANCASTER
Materials and Structures Department, Royal Aircraft Establishment, Farnborough, Hants, GU14 6TD, UK

The effect of plasticization on the ductile-to-brittle fracture transitions (DBFT) in the ball indentation of poly(ethersulphone) (PES) and poly(methyl methacrylate) (PMMA) has been studied. The DBFT in various organic liquids are governed by a size effect related to the indenter radius, in accordance with the Puttick theory of fracture transitions. In addition, abrasive wear rates of the polymers in these liquids are shown to correlate with the critical indenter radius needed to produce a fracture transition, owing to the connection with fracture toughness.

1. Introduction

Size effects are inherent in the energy rate-balance theory for fracture, since the volume strain energy available for fracture grows as the cube of some characteristic dimension, while the energy required for fracture increases only as the square of that dimension [1]. This causes transitions in deformation behaviour in that the stresses for elastic fracture or elastoplastic fracture may be greater than, or smaller than, the stress for widespread yielding, depending on the size of the cracked body and the mechanical properties of the material from which it is made [2]. Transitions are controlled by the relative values of a characteristic scaling length x and the material group $(K_c/\sigma_y)^2$ (or ER/σ_y^2) where K_c is the critical stress intensity factor for fracture, σ_y is the flow stress, E is Young's modulus and R is the specific work of fracture. At a deformation transition

$$x = \alpha\left(\frac{K_c}{\sigma_y}\right)^2$$

where α takes different values for different cracked geometries, depending on whether the transition is between elastic fracture and elastoplastic flow or elastoplastic fracture and plastic flow [3]. Puttick [3] termed these "lower" and "upper" transitions, respectively; there is a third transition from fully plastic flow to plastic fracture [2], but that is not relevant to the present investigation.

Clearly a change of size (x) alone will put bodies in various ranges $\gtrless\alpha(K_c/\sigma_y)^2$. Thus elastic (brittle) fracture occurs in large enough bodies made of ductile materials, since a sufficient increase in size can lower the fracture stress below the yield stress; vice versa it is difficult to comminute powders below certain sizes. Alternatively, at a fixed size, a change of one or more of the mechanical property parameters in $(K_c/\sigma_y)^2$ can cause transitions. Mechanical property changes may be effected by changes of rate, temperature or environment; the Charpy transition is a well-known example of this means of inducing altered behaviour. A review of such transitions has recently been given by Atkins and Mai [4].

In the case of indentation hardness, Roesler [5] first indicated the importance of scaling effects and transitions in connection with the initiation of Hertzian cracking in inorganic glass. He resolved Auerbach's 1891 observation [6] that the critical stress for cone cracking beneath a ball indenter decreased with increasing indenter radius. Although this and similar results had been explained away on the basis of a statistical distribution of sizes of natural flaws in the glass, Roesler showed that all the data satisfied a condition of constant strain energy just before fracture. Puttick and Yousif [7] studied ductile-to-brittle transitions in ball indentations in poly(methyl methacrylate) (PMMA) and determined the appropriate values for α at the transitions. For indentation fracture with spherical indenters, the lower transition for fracture in the elastic range is associated with the formation of a Hertzian-type ring crack, and the critical characteristic length for this fracture transition is the ring-crack radius. There exists a range of upper transitions from elastoplastic indentation flow to elastoplastic fracture, depending on the extent of the deformation field [3]. However, it is convenient to define the upper transition in terms of the formation of radial cracking when the ball reaches a depth of one full radius R, since this produces the maximum size of plastic zone; beyond this, we have deep punching. The

* *Present address*: IDM Electronics Ltd, 30 Suttons Park Avenue, Reading RG6 1AZ, UK.

0022–2461/86 $03.00 + .12

critical characteristic length at this upper transition will now be given by the length of the plastic zone, which is proportional to the radius of the indenter.

In the present paper we investigate transitions produced in poly(ethersulphone) (PES) and PMMA when organic liquids alter the values of $(K_c/\sigma_y)^2$ of the indented material, and relate the behaviour to plasticization effects. Since abrasive wear (modelled as a process of micromachining) is indentation coupled with sideways traction, we go on to discuss the wear of these polymers in the same liquids with reference to their indentation behaviour. We show that it is possible to relate abrasive wear rates with the critical indenter radius at deformation transitions.

2. Experimental details

Specimens were cut from one-inch thick sheets of PMMA and PES, supplied by ICI, into blocks of dimensions 50 mm × 50 mm × 25.4 mm. To reduce any residual stresses left from the casting process, the PMMA specimens were annealed at 100° C ($T_g \simeq 120°$ C) for 48 h, as recommended by ICI [8] for PMMA. The manufacturers' recommended annealing temperature for the PES blocks was 170° C ($T_g \simeq 225°$ C) for 16 h. Sudden cooling of the specimens was avoided by allowing them to cool to room temperature overnight. The surfaces of both sets of specimens were already highly polished; thus no surface treatment was administered besides washing them in a detergent solution, followed by rinsing and drying with a soft lens tissue.

All the indentation tests were conducted at room temperature (~22° C) on a J.J. Instruments T22K testing machine. Displacement was obtained from lead screws which moved the crosshead of the machine. The test specimens rested on the platform of a compression cage that had one end attached to the frame base, and the other end fixed below a 20 kN load cell. It was possible to obtain crosshead speeds between 0.5 and 75 mm min^{-1}. Voltages proportional to the load and displacement were fed to a Bryan's chart recorder to determine the maximum depth of penetration and the maximum load achieved during indentation. After the prescribed indentation depth had been attained, the specimens were unloaded at the same rate.

TABLE I Liquids used in the indentation experiments

Liquid	Solubility parameter δ_s $(MN\,m^{-3})^{1/2}$
n-Hexane	14.9
n-Hexadecane	15.3
Cyclohexane	16.8
Carbon tetrachloride	17.6
Xylene	18.0
Toluene	18.2
Acetone	20.3
n-Propanol	24.4
Ethanol	26.0
Ethane-diol	29.9
Ammonia solution	33.4
Formamide	39.3
Water	47.9

Liquids shown in Table I were introduced into the indentation area from a clean glass syringe at the start of each test, and in cases where rapid evaporation occurred (e.g. acetone) more liquid was delivered from the syringe during the coarse of the indentation, so that the test area was always flooded. Laboratory-grade liquids were used without further purification. These particular liquids were chosen as they cover a wide range of solvent solubility parameter δ_s [9]. (δ_s gives an approximate measure of the intermolecular cohesion in the fluid.)

The sizes of all indentations were arranged to be considerably smaller than the size of the specimens, in order to ensure that boundary effects did not influence the results. In general, if the diameter of an impression created by an indentation is d, the distance of the impression from the edge of the specimen (or from another impression) was not less than $3d$ to $4d$. Similarly, the minimum thickness of the specimen should be approximately eight times the depth of the indentation, otherwise the indenter will "sense" the presence of the surface on which it rests [10]. In all cases the indented area was examined after unloading using a low-power optical microscope for evidence of crazing and cracking.

In order to investigate lower transitions, the materials have to remain in the elastic range, which means either relatively high strain rates, low temperatures or low imposed strains. Since the effective strain under a ball indentation is $0.2(d/D)$ (where d and D are the impression and indenter diameters, respectively) [11], low strains are achieved with large indenters and/or small impressions. Hence a set of seven steel ball bearings, with radii ranging from 5 to 12.5 mm, were employed and the depth of penetration in the series of experiments was limited to 15% of the radius of the indenting ball. Furthermore a strain rate of $35 \times 10^{-3}\,sec^{-1}$ was employed. For upper transitions, in contrast, elastoplastic flow is required and this was achieved with a series of balls with smaller radii (0.5 to 3.96 mm) and depths of indentation equal to a full ball radius, giving greater imposed strains. The strain rate was reduced to $3.3 \times 10^{-3}\,sec^{-1}$ by fixing the indentation time at 60 sec.

In order to examine the effect of plasticization on the measured indentation pressure H, environmentally-affected values of this parameter for PES and PMMA were determined from load–penetration plots. In all these experiments, a 2 mm radius ball was pushed to a full-radius penetration at a strain rate of $3.3 \times 10^{-3}\,sec^{-1}$, and the flooded specimens were then unloaded at the same rate. There are drawbacks in the measurements of polymer hardness from residual indentations owing to the substantial elastic recovery which takes place on unloading. To overcome this problem of elastic contraction, the *in situ* radius of indentation a_s was calculated from the depth of penetration under load h_s by using the Saggital formula

$$a_s = (2Rh_s - h_s^2)^{1/2}$$

The Meyer hardness [12] of PES and PMMA in the

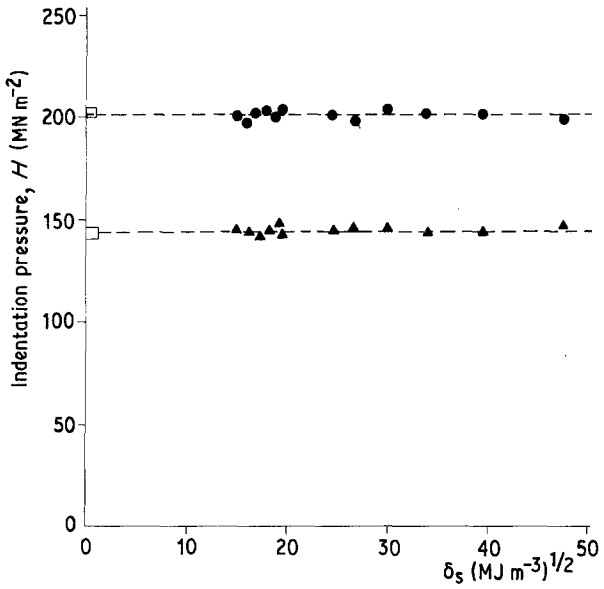

Figure 1 Variation of measured indentation pressure with δ_s for (▲) PES and (●) PMMA in various liquids, and (□) when dry.

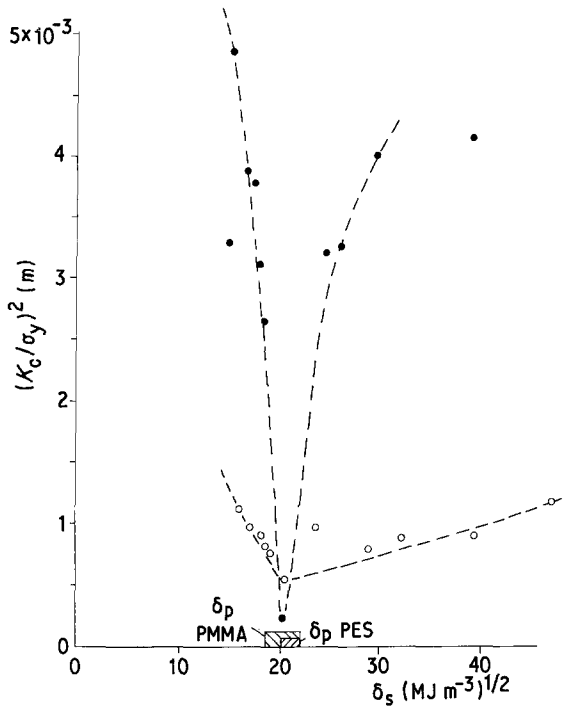

Figure 2 Variation of $(K_c/\sigma_y)^2$ with δ_s for (●) PES and (○) PMMA.

various environments is given by

$$H = L/\pi a_s^2$$

where L is the applied load.

3. Results and discussion

3.1. Bulk hardness and $(K_c/\sigma_y)^2$ parameter

Fig. 1 shows that the bulk hardness of PES and PMMA are essentially unaffected by plasticization effects produced by the organic liquids. These tests are useful as a relative measure of the indentation pressure in the presence of organic liquids, but for determining absolute values of indentation pressure, corrections must be made for the frictional force opposing the motion of the indenting ball. This was not attempted because the coefficient of friction between ball and specimen was not known.

The environmentally-affected material parameter $(K_c/\sigma_y)^2$ of PES and PMMA was estimated from the K_c values reported by Omar [13], and from other published data on σ_y. Since the bulk hardness of both these polymers was found to be unaffected by the different liquids, it was then reasonable to assume that the σ_y values would also be insensitive to them. For PES the yield stress (tensile) was taken as $\sigma_y = 84\,\mathrm{MN\,m^{-2}}$ [14], and for PMMA the yield stress (compressive) was taken as $\sigma_y = 130\,\mathrm{MN\,m^{-2}}$ [15]. These values of σ_y were taken at strain rates corresponding with those in the indentation tests. Fig. 2 reveals that plots of $(K_c/\sigma_y)^2$ against δ_s exhibit a minimum when $\delta_s \cong \delta_p$, which is most pronounced in the case of PES.

3.2. Indentation fracture

In many types of cracking experiments in polymers, it is often difficult to distinguish between crazes and cracks, particularly in the early stages of deformation. In the present series of experiments, intermittent crazing formed a "background" to all cracked indentations, particularly in the presence of liquids, although even in air faint crazes were observable. The orientation of the intermittent crazes followed the major stress system, i.e. circumferential at the lower transition determined by Hertzian ring cracking but radial at the upper transition determined by radial cracking. However, unlike the formation of true cracks, which was clearly size-dependent, craze formation in these experiments did not depend on size.

3.2.1. Upper fracture transitions

When PES and PMMA were indented with the series of increasing-size balls in dry conditions, there were no signs of cracking with indenters up to a radius of 1.97 mm. However, radial crazing and cracking were produced in PMMA using balls exceeding 1.97 mm in radius (e.g. Fig. 3). For PES, crack-free impressions were still obtained even after testing with the largest ball ($R = 3.96$ mm) which satisfied the depth requirements outlined in the previous section.

Indentation experiments were repeated on PES and PMMA with the surfaces of the blocks flooded with various liquids (listed in Table I). In these conditions, radial cracking readily occurred in both polymers with

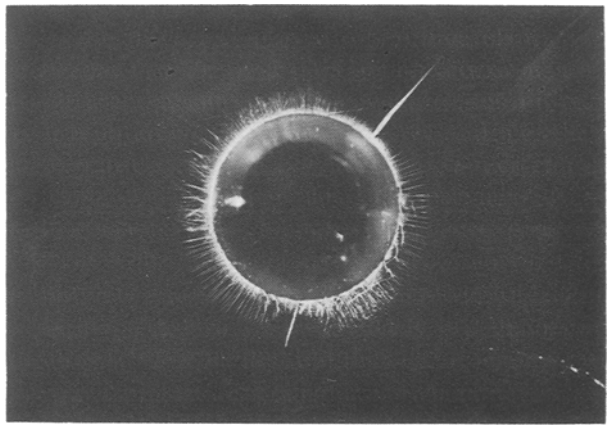

Figure 3 Radial cracks and crazes formed during loading of PMMA by a 1.97 mm stainless steel ball (dark field) (× 11).

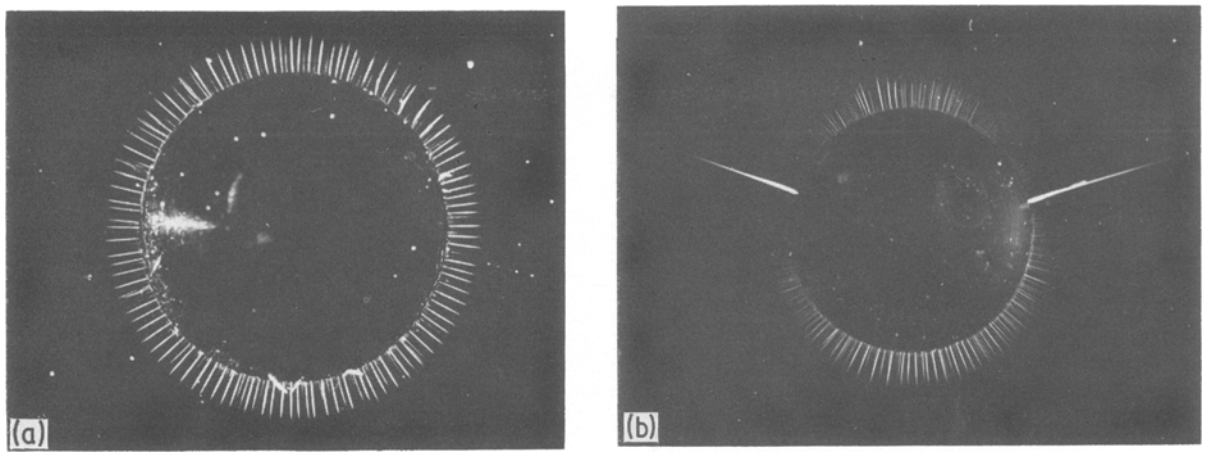

Figure 4 (a) Crazing pattern formed around an indentation in PES using a 2.15 mm radius stainless steel ball in the presence of cyclohexane (× 15). (b) Radial cracks formed in PES in the presence of cyclohexane using a 2.50 mm radius stainless steel ball (× 9).

the range of indenters. Moreover, since the liquids affect the toughness of the polymers to different extents, the transition from crack-free to cracked indentations was produced at different ball sizes in the various liquids. It was generally found that indentation tests performed with a relatively small indenter, in the presence of a given liquid, led to the formation of crazes in both PES and PMMA.* These crazes were observed as fine radial traces propagating outward from the periphery of the crater (Fig. 4a). With successively larger balls, there came a point when radial cracking was initiated around the impression (Fig. 4b).

In order to establish the influence of the liquids on the critical radius to fracture a_c, five tests were carried out with each polymer–liquid combination over the whole range of indenter sizes, and those producing radial cracks were counted. The statistical nature of crack formation precludes the existence of a sharp transition from ductile to brittle behaviour. Therefore, following Yousif [16], the upper fracture transition in each liquid was taken as the size of ball at which the percentage of uncracked specimens dropped below 100%. The results for both PES and PMMA, displayed in Figs 5a and b, show that the critical indenter radius a_c tends to a minimum when δ_s approaches δ_p. Independent measurements of K_{IC} in the presence of these liquids showed identical behaviour [13]. Maxwell and Rahm [17] proposed a plasticization theory to explain cracking or crazing in polymers in the presence of organic liquids which postulates that the stress-enhanced absorption of liquid into the polymer lowers the glass transition temperature of the stressed material causing cracking/crazing to occur at lower stresses. The ability of a liquid to plasticize a polymer depends on the difference in their respective values of solubility parameter; the smaller the difference the greater the degree of plasticization. The experimental results in Fig. 5 are in keeping with the plasticization theory. However, as with K_{IC}, not all the results for the whole spectrum of liquids fit a smooth curve when a_c is plotted against δ_s. This simply indicates that a more comprehensive parameter from the thermodynamics of mixing than the simple δ_s should be used to correlate these results. (For present purposes δ_s serves merely as a reference to plot against.)

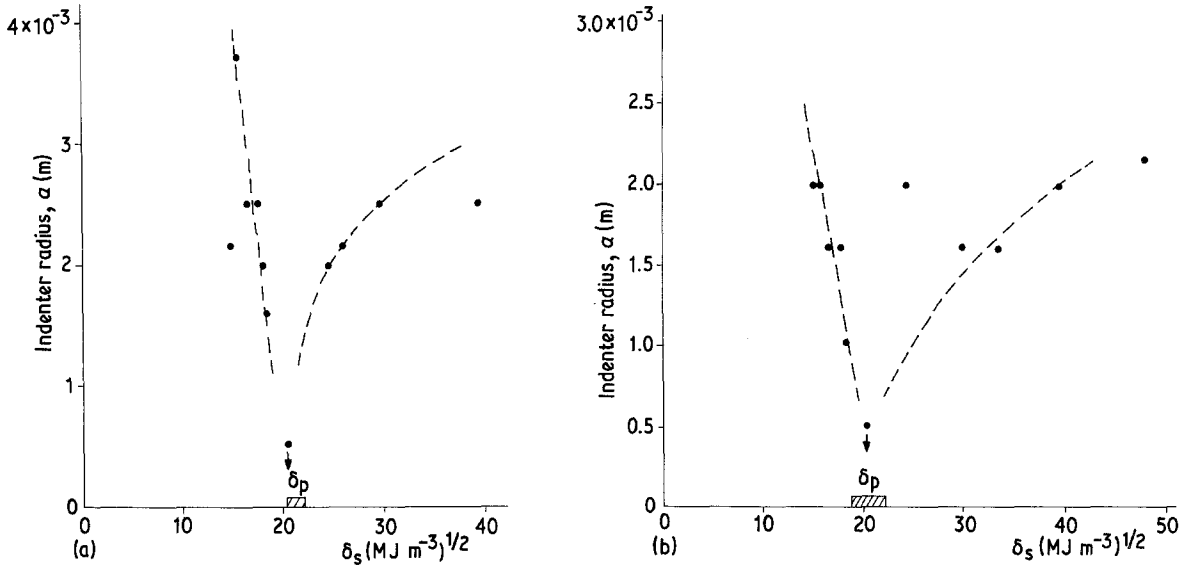

Figure 5 (a) A plot of indenter radius at the upper fracture transition against δ_s for PES. (b) A plot of indenter radius at the upper fracture transition against $\delta_s$for PMMA.

* Indentation experiments on PES and PMMA in dry conditions, followed by the subsequent introduction of organic liquids to the recovered craters, led to radial crazing patterns. This was attributed to residual stresses [13].

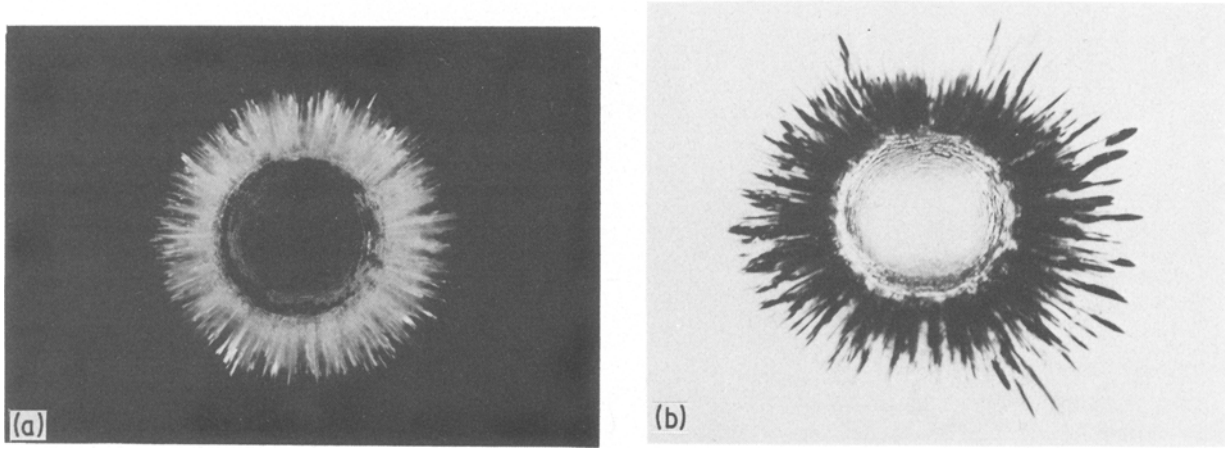

Figure 6 (a) Extensive radial cracking formed in PMMA in the presence of acetone using a 0.5 mm radius stainless steel ball (dark field) (× 29). (b) Extensive radial cracking formed in PES in the presence of acetone using a 0.5 mm radius stainless steel ball (bright field) (× 29).

Indentations conducted on PES and PMMA in the presence of acetone produced extensive radial cracking, even with the smallest indenter (R = 0.5 mm) (Figs 6a and b). This liquid has the most deleterious influence on the toughness of these polymers because it has the lowest value of $|\delta_s - \delta_p|$, and hence the greatest plasticizing effect. Experimental limitations prevented a smaller ball from being used to determine a_c because the lowest speed available to eliminate the effect of strain rate on the yield stress was 0.5 mm min^{-1}. To signify that the fracture transitions would actually occur with a ball of radius less than 0.5 mm for both PES and PMMA immersed in acetone, a downward arrow is drawn from these points in Fig. 5. It is interesting to note that, in addition to radial crazes and cracks, closely-spaced circumferential cracks could also be observed in the craters of most of the environmentally-affected indentations (e.g. Fig. 6b). This is consistent with the existence of a field of radial tensile stress generated by interfacial frictional traction between the steel ball and the plasticized polymer [18]. These cracks presumably arise during the unloading sequence of the indentation process.

3.2.2. Lower fracture transitions

In dry conditions, a ring crack was formed on the surface of PMMA specimens with balls about 10 mm radius. No such cracking was observed in PES, even when the largest indenter (R = 12.5 mm) was used. In the presence of acetone, balls of radii 7.5 mm and upwards generated concentric circumferential cracks in PMMA (Fig. 7), and the same type of crack-pattern was produced in PES with indenters greater than 5 mm in radius. This behaviour implies that acetone reduces the quasi-static toughness of PES more than that of PMMA. Indentation tests carried out on PES and PMMA in the presence of the other liquids, when balls ranging from 7.5 to 12.5 mm in radius were used, resulted in a very faint series of intermittent circumferential cracks. However, these cracks were not prominent enough to be used as a measure of the lower fracture transition.

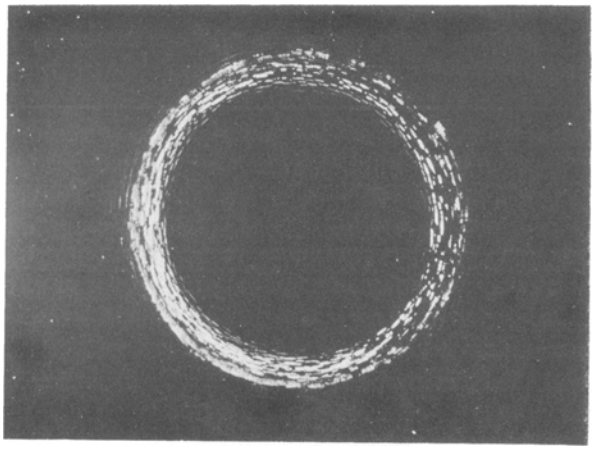

Figure 7 Circumferential cracking in PMMA whilst flooded by acetone. Depth of penetration = 0.15R. R = 7.5 mm (× 7).

3.3. Puttick's theory of indentation fracture transitions

It was shown earlier that the indenter radius required to produce an upper fracture transition decreases as δ_s tends to δ_p (Fig. 5). This dependency conforms with Puttick's theory of fracture transitions [3]. Furthermore, this theory predicts a quantitative relationship between the critical length for fracture and the "material length" $(K_c/\sigma_y)^2$ in the different environments, i.e. it predicts values of α in $x \gtrless \alpha(K_c/\sigma_y)^2$, where the size x is the plastic zone radius c associated with full penetration by a ball of radius R up to its waist, and which (according to Puttick [3]) is given by 1.65R. The slopes of c against $(K_c/\sigma_y)^2$ give α, which is expected to diminish with an increase in the magnitude of the tensile strain energy available for crack propagation. The gradients of the regressed lines in Figs 8a and b are 0.55 for PES and 1.64 for PMMA. These experimental results are much lower than the upper transition value given by Puttick's theory, which is 25. The discrepancies in slope may result from the interfacial frictional traction between the steel ball and the plasticized polymer, as evidenced by the circumferential cracks in the recovered craters (e.g. Fig. 6b). The additional force needed to overcome the frictional traction increases the tensile strain energy available for fracture, and leads to a correspondingly smaller critical characteristic length, i.e. a smaller α. In a more detailed analysis of Puttick's theory [3], it was

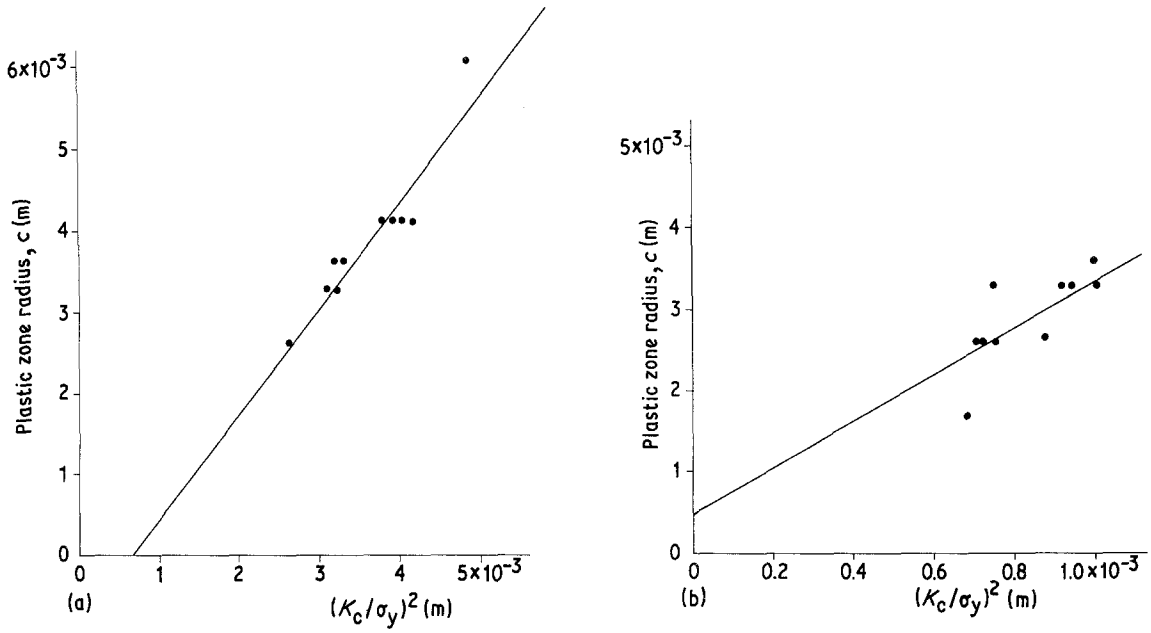

Figure 8 (a) Plastic zone radius at the upper fracture transition against $(K_c/\sigma_y)^2$ for PES (slope = 0.55, correlation coefficient = 0.93). (b) Plastic zone radius at the upper fracture transition against $(K_c/\sigma_y)^2$ for PMMA (slope = 1.64, correlation coefficient = 0.76).

hypothesized that α is dependent upon the size of the pre-existing flaw from which a crack propagates. It is therefore feasible that the differences in α between PES and PMMA can be ascribed to differences in inherent flaw size between the two polymers, as well as to possible differences in their interfacial frictional tractions.

3.4. The relationship between indentation fracture and abrasive wear

The existence of a size effect in indentation fracture has implications for many material-shaping and wear processes where particulate matter is removed via a microcutting mechanism, e.g. abrasion, grinding and erosion. Like indentation fracture, all these processes are closely bound up with the manner in which small-scale fractures initiate and propagate within highly localized stress fields. In a review of indentation fracture, Lawn and Wilshaw [19] suggest that macroscopic properties, such as the rate of abrasive wear of brittle materials, might be regarded as the summation of a large number of discrete indentation fracture "tests".

One way of relating abrasive wear to indentation experiments is to recall that the critical radius of an indenter which produces at least one radial fracture gives a relative measure of $(K_c/\sigma_y)^2$ – the "brittleness" of the indented body [3]. It has recently been hypothesized that for given asperity geometry, frictional conditions and load, the foregoing term dictates the transition from ploughing to microcutting when a abrading asperity traverses a surface [2]. Moreover, it has been proposed that increases in $(K_c/\sigma_y)^2$ would lead to an increased resistance to abrasion [20]. Therefore, in principle, it should be possible to conduct a series of indentation fracture experiments on a wide range of materials, or on the same material under different conditions, with the specific intention of correlating the indenter radius (a_c) at a fracture transition with the corresponding abrasive wear rates. Fig. 9 shows a graph of the abrasive wear rates of PMMA in a wide range of organic liquids, given by Omar [13], plotted against the critical indenter radius which produces at least one radial fracture in PMMA, in the presence of the same group of liquids. As expected, there is an inverse correlation between the two quantities, i.e. the abasive wear resistance diminishes with decreasing values of a_c. Because of the ease and rapidity of indentation testing, it may thus serve as a convenient technique for predicting the relative rate of abrasive wear for brittle materials.

4. Conclusions

Environmentally-affected indentation fracture experiments have been performed on PES and PMMA

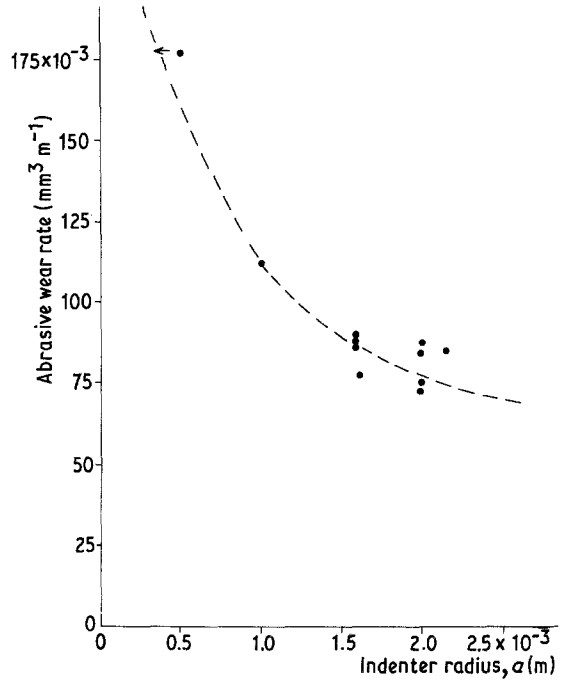

Figure 9 Abrasive wear rates of PMMA in various organic liquids [13] against the indenter radius at the upper fracture transition for PMMA in the same liquids.

using indenters of varying size. It has been found that the critical indenter radius a_c to produce at least one radial fracture correlates with the solvent solubility parameter δ_s, exhibiting a minimum when δ_s approaches δ_p, the solubility parameter of the polymer. Such a dependence conforms with Puttick's theory of fracture transitions.

The bulk hardness of PES and PMMA was shown to be comparatively unaffected by plasticization, and thus changes in $(K_c/\sigma_y)^2$ mainly reflect changes in K_c.

It has also been shown that abrasive wear rates, measured in a wide range of organic liquids, are inversely related to a_c, measured in the same liquids. Indentation fracture tests may therefore be used as a convenient technique to predict the relative rates of abrasive wear of brittle materials.

Acknowledgement

One of the authors (M.K.O.) is indebted to the Science and Engineering Research Council for the provision of a grant.

References

1. C. GURNEY and J. HUNT, *Proc. R. Soc.* **A299** (1967) 291.
2. A. G. ATKINS and Y. W. MAI, "Elastic and Plastic Fracture" (Ellis Horwood/John Wiley, Chichester, 1985).
3. K. E. PUTTICK, *J. Phys. D: Appl. Phys.* **13** (1980) 2249.
4. A. G. ATKINS and Y. W. MAI, *J. Mater. Sci.* (in press).
5. F. C. ROESLER, *Proc. Phys. Soc.* **B69** (1956) 55.
6. E. AUERBACH, *Ann. Phys. Chem.* **43** (1891) 61.
7. K. E. PUTTICK and R. H. YOUSIF, *J. Phys. D: Appl. Phys.* **16** (1983) 621.
8. Technical report PX122 (Imperial Chemical Industries, London).
9. J. BRANDRUP and E. H. IMMERGUT, "Polymer Handbook", 2nd Edn (1974).
10. D. TABOR, *Rev. Phys. Tech.* **1** (1970) 145.
11. *Idem*, "The Hardness of Metals" (Oxford University Press, 1951).
12. E. MEYER, *Z.D. Ver. Deut. Ing.* **52** (1908) 645.
13. M. K. OMAR, PhD thesis, University of Reading (1984).
14. L. S. A. SMITH and F. B. STANBRIDGE, in Proceedings of meeting on Physical Aspects of Polymer Science, University of Reading (Institute of Physics, London, 1983).
15. P. B. BOWDEN, in "Physics of Glassy Polymers", edited by R. N. Haward (Applied Science, 1973).
16. R. H. YOUSIF, PhD thesis, University of Surrey (1981).
17. B. MAXWELL and L. F. RAHM, *Ind. Eng. Chem.* **41** (1949) 1988.
18. K. L. JOHNSON, J. J. O'CONNOR and A. C. WOODWARD, *Proc. R. Soc.* **A334** (1973) 95.
19. B. R. LAWN and T. R. WILSHAW, *J. Mater. Sci.* **10** (1975) 1049.
20. A. G. ATKINS *Wear* **61** (1980) 183.

Received 29 July
and accepted 18 September 1985